

# Heterologous Expression of Fluostatin Gene Cluster Leads to a Bioactive Heterodimer

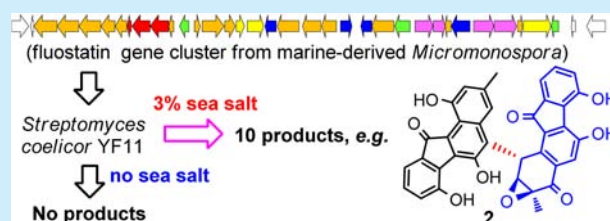
Chunfang Yang,<sup>†,‡</sup> Chunshuai Huang,<sup>†,‡</sup> Wenjun Zhang,<sup>\*,†</sup> Yiguang Zhu,<sup>†</sup> and Changsheng Zhang<sup>\*,†</sup>

<sup>†</sup>Key Laboratory of Tropical Marine Bio-resources and Ecology, Guangdong Key Laboratory of Marine Materia Medica, RNAM Center for Marine Microbiology, South China Sea Institute of Oceanology, Chinese Academy of Sciences, 164 West Xingang Road, Guangzhou 510301, China

<sup>‡</sup>University of Chinese Academy of Sciences, 19 Yuquan Road, Beijing 100049, China

## Supporting Information

**ABSTRACT:** The biosynthesis gene cluster (*fls*) for atypical angucycline fluostatins was identified from the marine derived *Micromonospora rosaria* SCSIO N160 and was confirmed by gene knockouts and the biochemical characterization of a bifunctional oxygenase FlsO2. The absolute configuration of the key biosynthetic intermediate prejadomycin was determined for the first time by Cu K $\alpha$  X-ray analysis. Heterologous expression of the intact *fls*-gene cluster in *Streptomyces coelicolor* YF11 in the presence of 3% sea salts led to the isolation of two new compounds: fluostatin L (1) and difluostatin A (2). Difluostatin A (2), an unusual heterodimer, exhibited antibacterial activities.



Fluostatins belong to the family of atypical angucyclines and contain a fluorenone chromophore with a unique 6–5–6–6 carbon ring skeleton.<sup>1</sup> A similar skeleton is also found in kinamycins<sup>2</sup> and lomaiviticins.<sup>3</sup> Until now, 11 fluostatins have been reported, including fluostatins A–E from *Streptomyces* species,<sup>4</sup> fluostatins F–H discovered by a culture-independent metagenomic approach,<sup>5</sup> and fluostatins I–K from the marine-derived *Micromonospora rosaria* SCSIO N160.<sup>6</sup> Fluostatins were found to exhibit varying degrees of dipeptidyl peptidases inhibition,<sup>4a</sup> antitumor,<sup>4b</sup> and antibacterial activities.<sup>5</sup>

The unique structures and bioactivities of fluostatins, kinamycins, and lomaiviticins have spurred great interest in total synthesis efforts.<sup>7</sup> Recently, a growing number of studies have been carried out to investigate the biosynthesis of kinamycins and lomaiviticins<sup>8</sup> and have led to the identification of their biosynthetic gene clusters,<sup>9</sup> the characterization of key biosynthetic intermediates,<sup>10</sup> the discovery of a new strategy for starter unit generation,<sup>11</sup> and the demonstration of key enzymes involved in oxidative ring contraction and epoxidation.<sup>12</sup> In contrast, limited studies were available for the biosynthesis of fluostatins. A metagenomics approach targeting type II polyketide synthase (PKS) genes has enabled the identification of a putative fluostatin gene cluster from soil environmental DNAs and has led to the production of fluostatins in a heterologous host of *Streptomyces albus*.<sup>5</sup> The biosynthesis of fluostatins was also investigated by feeding with [1-<sup>13</sup>C] labeled acetate, suggesting that the 6–5–6–6 ring skeleton of fluostatins arose from a rabelomycin-like precursor by oxidative excision and subsequent ring rearrangement.<sup>5</sup> In this study, we report the identification and characterization of the fluostatin biosynthetic gene cluster (*fls*) from the marine-derived *M. rosaria* SCSIO N160. Heterologous expression of the gene cluster in

*Streptomyces coelicolor* YF11 led to the discovery of an unusual heterodimer of fluostatins.

A genome sequencing approach was utilized to facilitate the identification of the putative fluostatin biosynthetic gene cluster from *M. rosaria* SCSIO N160. After contig assembly and bioinformatics analyses, the putative fluostatin gene cluster (*fls*) was localized on a continuous DNA region of around 40 kb (GenBank accession number KT726162), which comprised 36 open reading frames (ORFs) (Figure 1). The *fls* gene cluster was proposed to span from *flsF* to *flsR3* by comparison with the fluostatin biosynthetic gene cluster captured from soil eDNAs,<sup>5</sup> given their high amino acid sequence identities ranging from 63% to 88% (Table S1). In contrast, the ORFs flanking both gene clusters encoded distinct proteins (Table S1). Both fluostatin biosynthetic gene clusters displayed almost the same genetic organization, except that three ORFs (*orf13*, *orf26*, and *orf27*) from the soil eDNAs were absent in the *fls* gene cluster (Figure S3, Table S1). The subsequent screening of the SuperCos1-based genomic library of *M. rosaria* SCSIO N160 with primer pairs *flsGEF/flsGER* (Table S3) led to the identification of 13 positive cosmids out of 3072 clones. The relative location of three positive cosmids (pCSG5000, pCSG5001, and pCSG5003) to the putative *fls* biosynthetic gene cluster (Figures 1 and S1) was determined by end-sequencing. The cosmid pCSG5003 was found to harbor the entire putative *fls* biosynthetic gene cluster (Figure S1).

To verify the involvement of the *fls*-cluster in fluostatin biosynthesis, two type II polyketide synthase (PKS)-encoding genes *flsB* ( $\beta$ -ketoacyl synthase) and *flsI* (polyketide cyclase)

Received: September 16, 2015

Published: October 14, 2015

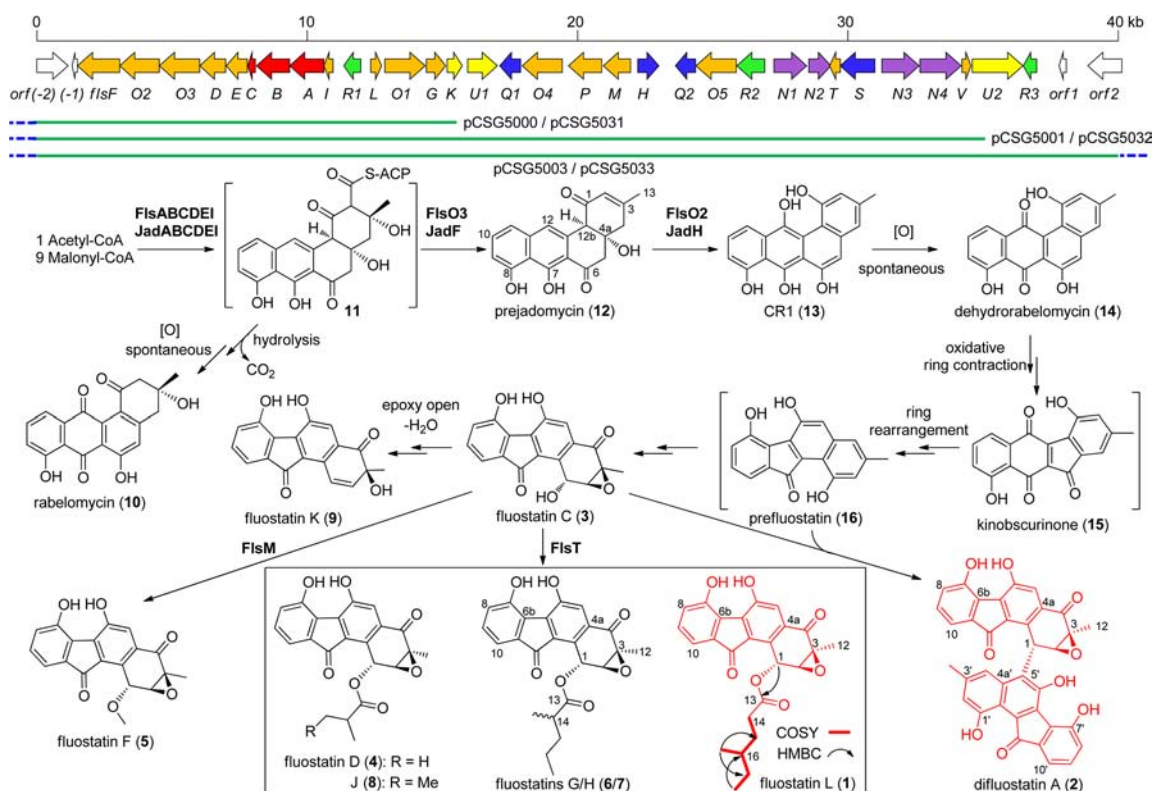


**Figure 1.** Genetic organization of the *fls*-gene cluster in *M. rosaria* SCSIO N160, relative location of positive cosmids, proposed biosynthetic pathway and structures of fluostatin analogues. Proposed functions of individual genes are provided in Table S1, and detailed information on cosmids are provided in Table S2.

were inactivated respectively by conventional PCR-targeted insertional mutagenesis (Figure S2). Both of the resulting mutants were unable to produce fluostatins (Figure S4). In contrast, the two mutants,  $\Delta orf[(-1)+(-2)]$  and  $\Delta orf(1+2)$  displayed the same production profile as that of the wild type strain (Figure S4), excluding their essential roles in fluostatin biosynthesis. The *flsO2* product resembles a number of well studied JadH-like bifunctional oxygenases involved in angucycline biosynthesis (Table S1).<sup>13</sup> The  $\Delta flsO2$  mutant displayed a distinct metabolite profile as that of wild type strain (Figure 2). Two products **12** (major) and **14** (minor) were isolated from the  $\Delta flsO2$  mutant and were identified as prejadomycin (**12**) and dehydrorabelomycin (**14**), respectively, by comparison of

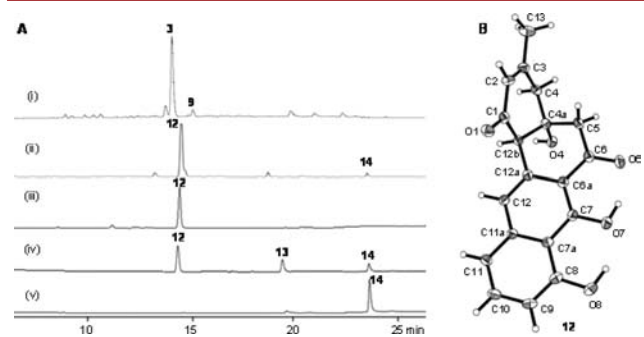


**Figure 2.** (A) HPLC analysis of metabolite profiles and enzyme assays of FlsO2. (i) *M. rosaria* SCSIO N160; (ii) the  $\Delta flsO2$  mutant; (iii) 100  $\mu$ M **12** incubated with 2 mM NADPH lacking FlsO2; (iv) 100  $\mu$ M **12** incubated with 5  $\mu$ M FlsO2 and 2 mM NADPH for 1.5 h at 28 °C; (v) 100  $\mu$ M **12** incubated with 5  $\mu$ M FlsO2 and 2 mM NADPH for 8 h at 28 °C. (B) X-ray crystal structure of prejadomycin (**12**).

HRESIMS and NMR spectroscopic data (Figure S5, Table S4) in literature.<sup>14</sup> By a single-crystal X-ray diffraction analysis using Cu  $K\alpha$  radiation with a Flack parameter value of  $-0.07(9)$ , the absolute configuration of **12** was confirmed for the first time as 4*a*R, 12*b*R (Figure 2B, Table S5). FlsO2 was confirmed by in vitro enzyme assays as a bifunctional enzyme, which was capable of completely converting **12** to **14** through the intermediate CR1 (**13**, *m/z* 322.4) (Figure 2A, traces iii–v; Figure S6). Similar catalytic properties have been previously described for JadH in jadomycin biosynthesis.<sup>13</sup> It should be noted that the  $\Delta flsO2$  mutant still accumulated a very minor amount of **14**, putatively due to the functional complementation of FlsO2 by other JadH-like oxygenases in the *fls*-gene cluster (such as FlsO1, FlsO4, and FlsO5; Table S1).

To further confirm that the cloned *fls*-gene cluster is intact, the recombinant plasmid pCSG5033 (Figure 1, Table S2), a derivative of the cosmid pCSG5003 that covers the entire putative *fls* biosynthetic gene cluster was introduced by conjugation into *S. coelicolor* YF11.<sup>15</sup> As controls, two plasmids harboring truncated *fls*-gene clusters, pCSG5031 (lacking *flsK*–*R3*) and pCSG5032 (lacking *flsU2* and *flsR3*) (Figure 1, Table S2), and the void vector pSET152, were also introduced into *S. coelicolor* YF11. Considering that *M. rosaria* SCSIO N160 required sea salts for producing fluostatins,<sup>6</sup> sea salts were also added to culturing media in the heterologous host. Interestingly, no products were observed from *S. coelicolor* YF11/pCSG5033 without the supplement of sea salts (Figure 3, trace i). Production of more fluostatins was observed when adding more sea salts (Figure 3, traces ii–iv), and a number of fluostatin analogues were produced when supplementing with 3% sea salts (Figure 3, trace iv). However, even with adding 3% sea salts, the two *S. coelicolor* strains harboring the void vector pSET152 and

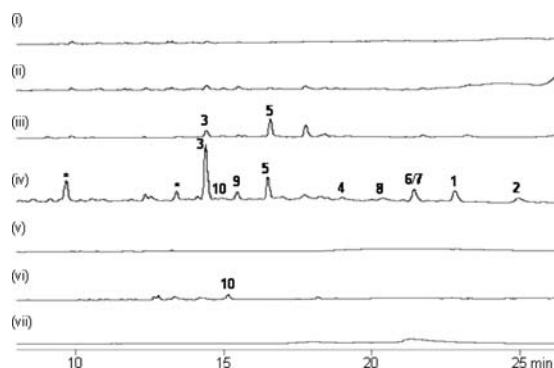


**Figure 3.** HPLC analysis of metabolite profiles of heterologous expression of *fls*-gene cluster in *S. coelicolor* YF11. *S. coelicolor* YF11/pCSG5033 cultured with sea salts (i) 0%, (ii) 1%, (iii) 2%, (iv) 3%; *S. coelicolor* YF11 harboring (v) pSET152, (vi) pCSG5031, and (vii) pCSG5032 cultured with 3% sea salts. The symbol \* denotes uncharacterized products.

pCSG5032 (containing the truncated *fls* gene cluster lacking *flsU2-flsR3*) produced no fluostatins (Figure 3, traces v, vii), while another *S. coelicolor* YF11 strain harboring pCSG5031 (containing *flsF-flsG*) only produced a very minor amount of rabelomycin (10) (Figure 3, trace vi).

A large scale of fermentation of *S. coelicolor* YF11/pCSG5033 in 3% sea-salt-containing media led to the isolation of fluostatin analogues 1–10. The known compounds fluostatins C (3), D (4), F (5), G/H (6/7), J (8), K (9), and rabelomycin (10) were characterized by comparing their spectroscopic data (data not shown) with those previously reported.<sup>5,6</sup> Fluostatin L (1) was obtained as a red powder. The molecular formula of 1 was established as  $C_{25}H_{24}O_7$  ( $m/z$  435.1448 [M – H]<sup>–</sup>, calcd 435.1449) by HRESIMS. The comparison of <sup>1</sup>H and <sup>13</sup>C NMR spectroscopic data for 1 (Table S6, Figure S7) and fluostatin J (8)<sup>6</sup> suggested the presence of a 4-methyl-hexaoyloxy group in 1. This assignment was supported by HMBC correlations (Figure S7) from H<sub>3</sub>-19 to C-15/C-16/C-17, from H<sub>3</sub>-18 to C-16/C-17, and from H-14 to C-13 (Figure 1). A *trans* configuration between H-1 and H-2 in 1 was indicated by the *J* value of H-1/H-2 (<sup>3</sup>*J*<sub>H1–H2</sub> 2.0 Hz). The absolute configurations of C-1, C-2, and C-3 in 1 were assigned as 1*R*, 2*S*, and 3*S* by comparing the experimental circular dichroism spectra of 1 and 3 (Figure S8).<sup>6</sup> However, the configuration at C-16 has remained elusive. Difluostatin A (2) was isolated as a dark red powder. The molecular formula of 2 was established as  $C_{36}H_{22}O_9$  ( $m/z$  597.1191 [M – H]<sup>–</sup>, calcd 597.1180). The <sup>1</sup>H, <sup>13</sup>C, and HSQC NMR data for 2 displayed two singlet methyls, nine sp<sup>2</sup> methines, two sp<sup>3</sup> methines, and two exchangeable protons (Table S6, Figure S9). The COSY spectrum (Figure S9-D) of 2 revealed two groups of characteristic aromatic ABC spin systems ( $\delta_H$  7.07/7.34/7.33 and  $\delta_H$  7.02/7.22/7.18, Table S6, Figure S9), indicating that 2 was a heterodimer. Two ions at  $m/z$  291 and 306 acquired in the MS/MS analysis of 2 provided further evidence for a dimer (Figure S9-A). Careful analysis of COSY and HMBC (Figure S9) correlations allowed the construction of the units A and B in 2 (Figure 4). The connection of units A and B through C-1 and C-5' were determined by HMBC correlations from H-1 to C-4a'/C-5', from H-2 to C-5', and from H-4' to C-4a'/C-5' and the NOESY correlation between H-1 and H-4' (Figure 4 and Figure S9). Thus, the planar structure of 2 (Figure 1) was established as a C–C coupled heterodimer linked by C-1 of 3 and C-5' of prefluostatin (16), a putative intermediate of

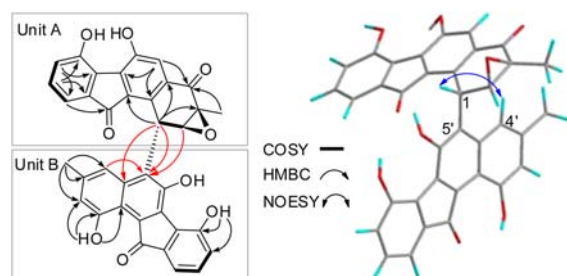


**Figure 4.** Key HMBC, COSY, and NOESY correlations for 2. Key correlations connecting units A and B are in red.

kinamycin biosynthesis in *Streptomyces*.<sup>16</sup> The *trans* configuration between H-1 and H-2 in 2 was indicated by the *J* value of H-1/H-2 (<sup>3</sup>*J*<sub>H1–H2</sub> 4.0 Hz). Finally, the absolute configuration of 2 was tentatively assigned as 1*S*, 2*S*, and 3*S* upon considering its biosynthetic origin from 3 (Figure 1).

Next, compounds 1–10, 12, and 14 were assayed for antibacterial activities against four indicator strains including *Klebsiella pneumonia* ATCC 13883, *Aeromonas hydrophila* ATCC 7966, *Staphylococcus aureus* ATCC 29213, and *Enterococcus faecalis* ATCC 29212, using trimethoprim (TMP) as a positive control. Compounds 1, 3–9 had negligible activities with minimal inhibition concentration (MIC) values >64  $\mu\text{g mL}^{-1}$ . Interestingly, difluostatin A (2) displayed antibacterial activities against three indicator strains with MIC values of 4–8  $\mu\text{g mL}^{-1}$ , and 2 exhibited better activity than 12 and 14 against *S. aureus* (Table 1). In contrast, the monomer 3 had no antibacterial

**Table 1.** Antibacterial Activities of Fluostatin Analogues

	MIC ( $\mu\text{g mL}^{-1}$ )			
	<i>K. pneumonia</i> ATCC 13883	<i>A. hydrophila</i> ATCC 7966	<i>S. aureus</i> ATCC 29213	<i>E. faecalis</i> ATCC 29212
2	4	4	8	>64
10	4	4	16	16
12	16	8	>64	>64
14	1	1	16	>64
TMP	0.25	0.25	4	2

activities. In a recent study, it was found that the dimer lomaiviticin A was more cytotoxic to human cancer cells than the monomers lomaiviticin C and kinamycin C.<sup>17</sup>

On the basis of our experimental data and bioinformatics analysis, a plausible biosynthetic pathway for fluostatins was proposed (Figure 1). A type II PKS system (FlsABCDEI), analogous to that established in the jadomycin pathway,<sup>18</sup> would lead to an intermediate 11, undergoing either spontaneous hydrolysis and oxidation to the shunt product 10, or FlsO3-catalyzed formation of prejadomycin (12). Then, FlsO2 catalyzed the conversion of 12 to 14 through CR1 (13). The oxidative ring opening of 14 to form the putative intermediate kinobscurinone (15) might involve FlsG, analogous to well studied enzyme AlpJ in the kinamycin pathway that catalyzed similar reactions.<sup>12a</sup> The conversion of 15 to prefluostatin (16), an intermediate deduced from difluostatin A (2), was similar to a complicated ring rearranging process that was recently speculated in lomaiviticin biosynthesis.<sup>9c</sup> This process was hypothesized to be concomitant with diazo-formation in lomaiviticin biosynthesis involving a conserved set of enzymes that were also found in fluostatins (FlsT, FlsS, FlsN3, FlsN4, FlsV, and FlsU2).<sup>9c</sup> Subsequently, tailoring oxidative modifica-

tions of **16** would generate the major product fluostatin C (**3**). The methylation of **3** by FlsM afforded **5**, and the flexible acylation of **3** by FlsT led to diversified products **1**, **4**, **6–8**. Fluostatin K (**9**) was proposed to be derived from **3** by opening of the epoxy ring (probably catalyzed by FlsH, an analogue of established epoxy hydrolases Alp1U and Lom6<sup>12b</sup>) and a following dehydration. The coupling of **3** and **16**, in a not yet understood manner, would lead to the heterodimer difluostatin A (**2**).

C–C coupled symmetric natural product homodimers are often encountered in nature,<sup>19</sup> such as actinorhodin (C10–C10'),<sup>20</sup> himastatin (C5–C5'),<sup>21</sup> julichrome Q (C7–C7'),<sup>22</sup> and lomaiviticin A (C2–C2').<sup>9b,c</sup> However, difluostatin A (**2**) represents a rare example of an asymmetric heterodimer with a C1–C5' coupling.<sup>23</sup> The C–C bond formations in himastatin and julichrome have been demonstrated to be mediated by P450 enzyme-catalyzed biaryl coupling.<sup>21,22</sup> The FlsQ1 homologues, ActVA-orf4,<sup>20</sup> Lom19,<sup>9b</sup> and Strop2191,<sup>9c</sup> belonging to the NmrA family of regulatory proteins, have been implicated as dimerization enzymes in actinorhodins and lomaiviticins. Thus, FlsQ1 might play an important role in the formation of **2**.

## ■ ASSOCIATED CONTENT

### Supporting Information

The Supporting Information is available free of charge on the ACS Publications website at DOI: 10.1021/acs.orglett.5b02683.

Experimental procedures, characterization data for compounds (PDF)

X-ray crystallization data for **12** (CIF)

## ■ AUTHOR INFORMATION

### Corresponding Authors

\*E-mail: wzhang@scsio.ac.cn.

\*E-mail: czhang2006@gmail.com.

### Notes

The authors declare no competing financial interest.

## ■ ACKNOWLEDGMENTS

Financial support was provided by NSFC (31125001 and 31290233), Guangdong Province (2015A030308013, GD2012-D01-002, GD2012-D01-001), and Chinese Academy of Sciences (XDA11030403). We are grateful to the analytical facilities in SCSIO.

## ■ REFERENCES

- (1) Kharel, M. K.; Pahari, P.; Shepherd, M. D.; Tibrewal, N.; Nybo, S. E.; Shaaban, K. A.; Rohr, J. *Nat. Prod. Rep.* **2012**, *29*, 264–325.
- (2) (a) Omura, S.; Nakagawa, A.; Yamada, H.; Hata, T.; Furusaki, A. *Chem. Pharm. Bull.* **1973**, *21*, 931–940. (b) Gould, S. J.; Tamayo, N.; Melville, C. R.; Cone, M. C. *J. Am. Chem. Soc.* **1994**, *116*, 2207–2208. (c) Mithani, S.; Weeratunga, G.; Taylor, N. J.; Dmitrienko, G. I. *J. Am. Chem. Soc.* **1994**, *116*, 2209–2210. (d) Proteau, P. J.; Li, Y. F.; Chen, J.; Williamson, R. T.; Gould, S. J.; Laufer, R. S.; Dmitrienko, G. I. *J. Am. Chem. Soc.* **2000**, *122*, 8325–8326.
- (3) (a) He, H.; Ding, W. D.; Bernan, V. S.; Richardson, A. D.; Ireland, C. M.; Greenstein, M.; Ellestad, G. A.; Carter, G. T. *J. Am. Chem. Soc.* **2001**, *123*, 5362–5363. (b) Woo, C. M.; Beizer, N. E.; Janso, J. E.; Herzon, S. B. *J. Am. Chem. Soc.* **2012**, *134*, 15285–15288.
- (4) (a) Akiyama, T.; Harada, S.; Kojima, F.; Takahashi, Y.; Imada, C.; Okami, Y.; Muraoka, Y.; Aoyagi, T.; Takeuchi, T. *J. Antibiot.* **1998**, *51*, 553–559. (b) Baur, S.; Niehaus, J.; Karagouni, A. D.; Katsifas, E. A.; Chalkou, K.; Meintanis, C.; Jones, A. L.; Goodfellow, M.; Ward, A. C.;

Beil, W.; Schneider, K.; Sussmuth, R. D.; Fiedler, H. P. *J. Antibiot.* **2006**, *59*, 293–297.

(5) Feng, Z. Y.; Kim, J. H.; Brady, S. F. *J. Am. Chem. Soc.* **2010**, *132*, 11902–11903.

(6) Zhang, W. J.; Liu, Z.; Li, S. M.; Lu, Y. Z.; Chen, Y. C.; Zhang, H. B.; Zhang, G. T.; Zhu, Y. G.; Zhang, G. Y.; Zhang, W. M.; Liu, J. S.; Zhang, C. S. *J. Nat. Prod.* **2012**, *75*, 1937–1943.

(7) (a) Yu, M.; Danishefsky, S. J. *J. Am. Chem. Soc.* **2008**, *130*, 2783–2785. (b) Nicolaou, K. C.; Li, H.; Nold, A. L.; Pappo, D.; Lenzen, A. J. *Am. Chem. Soc.* **2007**, *129*, 10356–10357. (c) Lei, X.; Porco, J. A., Jr. *J. Am. Chem. Soc.* **2006**, *128*, 14790–14791. (d) Herzon, S. B.; Lu, L.; Woo, C. M.; Gholap, S. L. *J. Am. Chem. Soc.* **2011**, *133*, 7260–7263.

(8) Gould, S. J. *Chem. Rev.* **1997**, *97*, 2499–2510.

(9) (a) Gould, S. J.; Hong, S. T.; Carney, J. R. *J. Antibiot.* **1998**, *51*, 50–57. (b) Kersten, R. D.; Lane, A. L.; Nett, M.; Richter, T. K. S.; Duggan, B. M.; Dorrestein, P. C.; Moore, B. S. *ChemBioChem* **2013**, *14*, 955–962. (c) Janso, J. E.; Haltli, B. A.; Eustaquio, A. S.; Kulowski, K.; Waldman, A. J.; Zha, L.; Nakamura, H.; Bernan, V. S.; He, H.; Carter, G. T.; Koehn, F. E.; Balskus, E. P. *Tetrahedron* **2014**, *70*, 4156–4164.

(10) (a) Gould, S. J.; Melville, C. R. *Bioorg. Med. Chem. Lett.* **1995**, *5*, 51–54. (b) Gould, S. J.; Melville, C. R.; Cone, M. C.; Chen, J.; Carney, J. R. *J. Org. Chem.* **1997**, *62*, 320–324. (c) Woo, C. M.; Gholap, S. L.; Herzon, S. B. *J. Nat. Prod.* **2013**, *76*, 1238–1241.

(11) Waldman, A. J.; Balskus, E. P. *Org. Lett.* **2014**, *16*, 640–643.

(12) (a) Wang, B.; Ren, J.; Li, L.; Guo, F.; Pan, G.; Ai, G.; Aigle, B.; Fan, K.; Yang, K. *Chem. Commun.* **2015**, *51*, 8845–8848. (b) Wang, B.; Guo, F.; Ren, J.; Ai, G.; Aigle, B.; Fan, K.; Yang, K. *Nat. Commun.* **2015**, *6*, doi:10.1038/ncomms8674.

(13) Chen, Y. H.; Wang, C. C.; Greenwell, L.; Rix, U.; Hoffmeister, D.; Vining, L. C.; Rohr, J. R.; Yang, K. Q. *J. Biol. Chem.* **2005**, *280*, 22508–22514.

(14) (a) Rix, U.; Wang, C.; Chen, Y.; Lipata, F. M.; Remsing Rix, L. L.; Greenwell, L. M.; Vining, L. C.; Yang, K.; Rohr, J. *ChemBioChem* **2005**, *6*, 838–845. (b) Seaton, P. J.; Gould, S. J. *J. Am. Chem. Soc.* **1987**, *109*, 5282–5284.

(15) Zhou, H.; Wang, Y.; Yu, Y.; Bai, T.; Chen, L.; Liu, P.; Guo, H.; Zhu, C.; Tao, M.; Deng, Z. *Curr. Microbiol.* **2012**, *64*, 185–190.

(16) Yao, C. B. F.; Schiebel, M.; Helmke, E.; Anke, H.; Laatsch, H. Z. *Naturforsch., B: J. Chem. Sci.* **2006**, *61*, 320–325.

(17) Colis, L. C.; Woo, C. M.; Hegan, D. C.; Li, Z. W.; Glazer, P. M.; Herzon, S. B. *Nat. Chem.* **2014**, *6*, 504–510.

(18) Fan, K.; Pan, G.; Peng, X.; Zheng, J.; Gao, W.; Wang, J.; Wang, W.; Li, Y.; Yang, K. *Chem. Biol.* **2012**, *19*, 1381–1390.

(19) Kozlowski, M. C.; Morgan, B. J.; Linton, E. C. *Chem. Soc. Rev.* **2009**, *38*, 3193–3207.

(20) (a) Okamoto, S.; Taguchi, T.; Ochi, K.; Ichinose, K. *Chem. Biol.* **2009**, *16*, 226–236. (b) Taguchi, T.; Ebihara, T.; Furukawa, A.; Hidaka, Y.; Ariga, R.; Okamoto, S.; Ichinose, K. *Bioorg. Med. Chem. Lett.* **2012**, *22*, 5041–5045.

(21) Ma, J.; Wang, Z.; Huang, H.; Luo, M.; Zuo, D.; Wang, B.; Sun, A.; Cheng, Y. Q.; Zhang, C.; Ju, J. *Angew. Chem., Int. Ed.* **2011**, *50*, 7797–7802.

(22) Prag, A.; Gruning, B. A.; Hackh, M.; Ludeke, S.; Wilde, M.; Luzhetskyy, A.; Richter, M.; Luzhetskya, M.; Gunther, S.; Muller, M. J. *Am. Chem. Soc.* **2014**, *136*, 6195–6198.

(23) Bringmann, G.; Gulder, T.; Gulder, T. A.; Breuning, M. *Chem. Rev.* **2011**, *111*, 563–639.